

We are IntechOpen, the world's leading publisher of Open Access books Built by scientists, for scientists

6,900

Open access books available

185,000

International authors and editors

200M

Downloads

Our authors are among the

154

Countries delivered to

TOP 1%

most cited scientists

12.2%

Contributors from top 500 universities



WEB OF SCIENCE™

Selection of our books indexed in the Book Citation Index
in Web of Science™ Core Collection (BKCI)

Interested in publishing with us?
Contact book.department@intechopen.com

Numbers displayed above are based on latest data collected.
For more information visit www.intechopen.com



Research and Development of the Passive Optoelectronic Rangefinder

Vladimir Cech¹ and Jiri Jevicky²

¹*Oprox, a.s., Brno*

²*University of Defence, Brno
Czech Republic*

1. Introduction

1.1 Basic specification of the problem

The topographical coordinates of an object of interest (the target), which is represented by one contractual point $T = (E, N, H)_T$, need to be determined indirectly in many cases that occur in practice, because an access to respectively the target and the target point T is disabled due to miscellaneous reasons at a given time. Hereafter we will confine to methods that make use of specialized technical equipment (rangefinders) to determine coordinates of the target point T - Fig. 1.

The point $P_{RF} = (E, N, H)_{RF}$ represents a contractual position of the rangefinder in the topographical coordinate system, D_T is the target slant range measured by means of the rangefinder. This value D_T represents the estimate of the real slant range of the target D_{T0} that is equal contractually to the distance of points P_{RF} and T . The angle ε_T is the measured estimate of the elevation of the target ε_{T0} and the angle a_T is the measured estimate of the target azimuth a_{T0} . The coordinates (D, ε, a) are relative spherical coordinates towards the contractual position of the rangefinder which is represented by the point P_{RF} .

The rangefinder is a device that, from the view of Johnson's criterion for optical systems classification, functions to locate the target (target coordinates $(E, N, H)_T$) and usually it also functions to determine motional parameters of the target that are primarily represented by the instantaneous target velocity vector \mathbf{v}_T - Fig. 2.

Typical measured ranges interval for ground targets is from 200 to 4000 m and for aerial or naval targets from 200 to 10000 m or more.

1.2 Passive optoelectronic rangefinder (POERF)

The passive optoelectronic rangefinder (POERF, Fig. 1, 8) is a measurement device as well as a mechatronic system that measures geographic coordinates of objects (targets) selected by an operator in real time (in online mode). In the case of a moving object, it also automatically evaluates its velocity vector \mathbf{v}_T and simultaneously extrapolates its trajectory - Fig. 2.

Active rangefinders for measurement of longer distances of objects (targets), e.g. pulsed laser rangefinders (LRF), emit radiant energy, which conflicts with hygienic restrictions in many applications and sometimes with given radiant pollutions limitations, too. In security and military applications there is a serious defect that the target can detect its irradiation. The use of POERF eliminates mentioned defects in full.

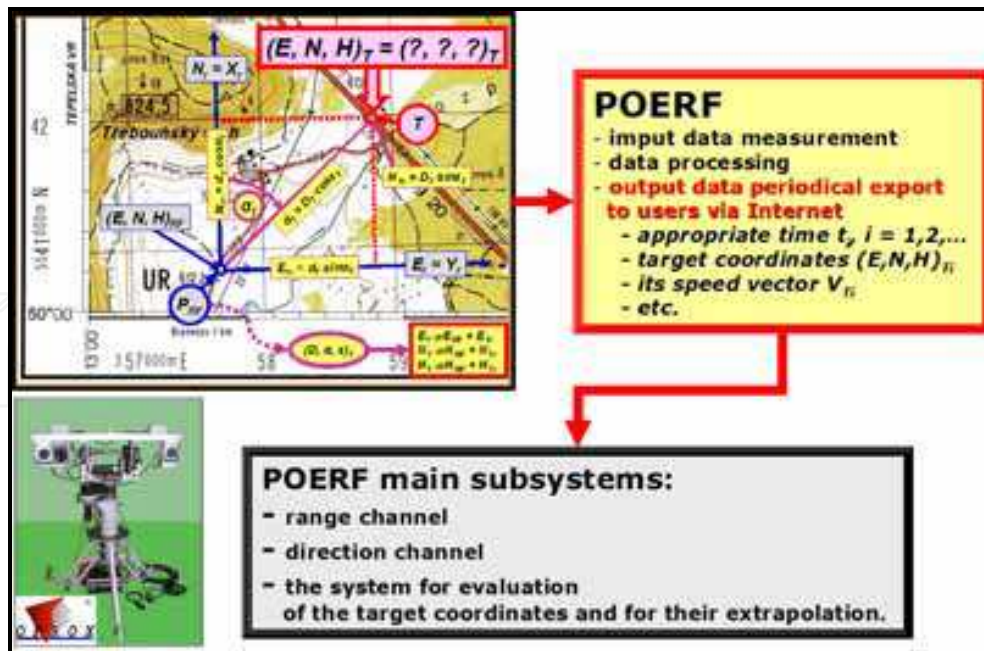


Fig. 1. Input/Output characteristics of POERF (the demonstration model 2009)

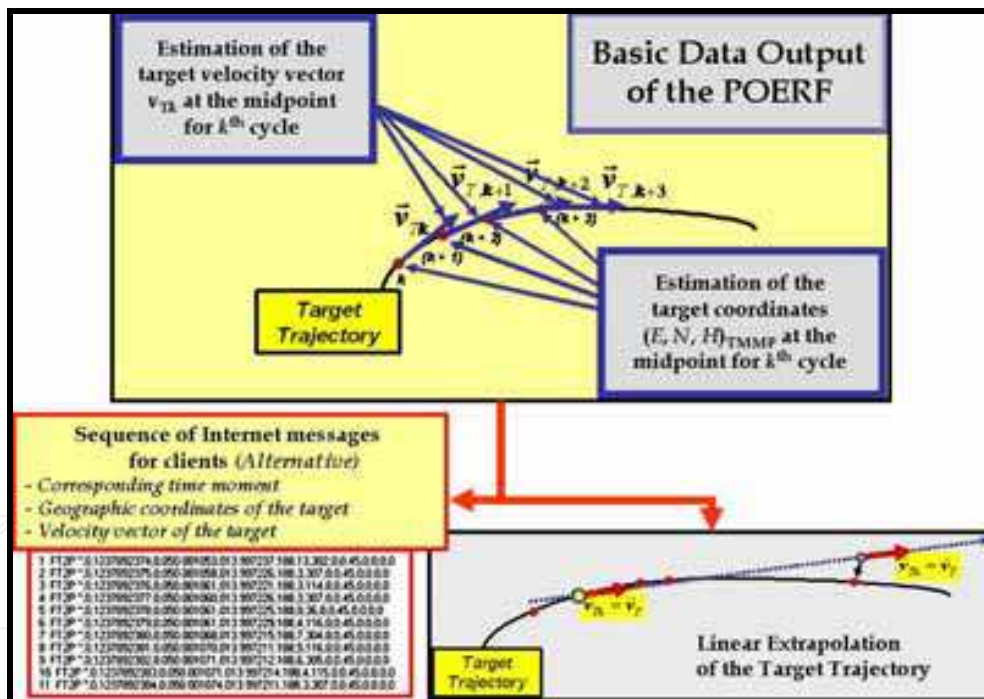


Fig. 2. Principle of measurement of the target trajectory and the data export to users (clients)

The POERF measurement principle is based on the evaluation of information from stereo-pair images obtained by the sighting (master) camera and the metering (slave) one (see the subsection 4.1 and the Figure 9). Their angles of view are relatively small and therefore a spotting camera with zoom is placed alongside the sighting camera – Fig. 1, 9. This spotting camera is exploited by an operator for targets spotting. After operator’s steering the cameras towards a target, the shots from the sighting camera serve to evaluate angle measured errors and to track the target automatically (see the section 3).

The POERF is able to work in two modes: online and offline (processing of images saved in memory - e.g. on the hard disc). The offline mode enables to measure the distance of fleeting targets groups in time lag to approx. 30 seconds. The active rangefinders are not able to work in a similar mode (see the section 2).

In general, the POERF continues to measure the UTM coordinates (Fig. 1, 2) of moving target with rate from 10 to 30 measurements per second and extrapolates its trajectory. All required information is sent to external users (clients) via the Internet in near-real-time whereas the communications protocol and the repetitive period (for example 1 s - Fig. 2) are preconcerted. The coordinates can be transformed to the coordinate system WGS 84 and sent to other systems - in accordance with the client's requirement.

Presumed users of the future system POERF are the police, security agencies (ISS - Integrated Security Systems, etc.) and armed forces (NATO NEC - the NATO Network Enabled Capability, etc.).

1.3 The state of POERF research and development, used methods and tools, results

1.3.1 Demonstration model of the POERF

A demonstration model of the POERF (Fig.1, 8) was presented to the opponent committee of the Ministry of Industry and Trade of the Czech Republic within the final opponent proceeding in March 2009. The committee stated that POERF is fully functional and recommended continuing in its further research and development. This chapter will give basic information about the research and development of this POERF demonstration model. The working range of measured distances is circa from 50 m to 1000 m at the demonstration model (see the subsection 4.1).

1.3.2 Simulation programs Test POERF, Test POERF RAW and the Catalogue of targets

In this chapter the basic possibilities of simulation program Test POERF (see the section 5) are presented. This program serves to simulate functions of the range channel core of the POERF. It allows verifying the quality of algorithms for a target slant range finding from taken stereo pair images of the target and its surroundings. These images are generated as a virtual reality by a special images generator in the program - Fig. 12.

Next, we present consequential simulation software package Test POERF RAW which works with taken images of a real scene (see the section 5, too). The package presently consists of three separate programs: the editing program RAWedi, the main simulation program RAWdis and the viewer RAWpro. The editor RAWedi allows editing of stereo pair images of individual targets and supports the creation of the Catalogue of targets. The simulation program RAWdis serves for testing algorithms for estimation of horizontal stereoscopic disparity (stereo correspondence algorithms) which are convenient for the use in POERF. Simulation experiments can also help to solve problems in the development process of the software for a future POERF prototype.

In publications that deal with problems of stereoscopic disparity determination there is constantly emphasized the deficiency of quality stereoscopic pairs of varied object images, which are indispensable to testing the functionality and quality of various algorithms under real conditions. Considering the POERF specifics, we have decided to create own database of horizontal stereo pair images of targets with accurately known geographic coordinates - shortly the "Catalogue of Targets" (see the section 5 and the Figures 16, 17).

The stationary “targets” (73 objects) were chosen, so that on the one hand they cover slant ranges from c. 100 m to c. 4000 m and on the other hand their appearance and placement should be convenient for unique determination of their stereoscopic disparity – Fig. 17. The number of successive stereo pair images of every target is minimally 512, which is precondition for statistical processing of simulation experiments results.

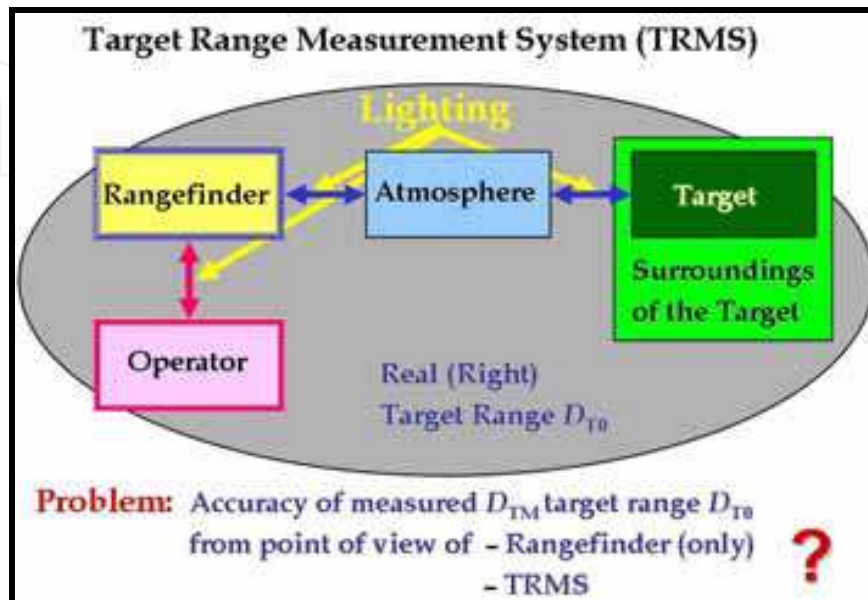


Fig. 3. Target Range Measurement System – TRMS

1.4 What has been done by other researchers

The principle of passive optoelectronic rangefinder has been known minimally since the 50's or 60's of the 20th century (see the subsection 3.1). The development was conditioned primarily by progress in the areas of digital cameras and in miniature computers with ability to work in field conditions (target temperature limit from -40 to $+50$ °C, dusty environment, etc.) and to realize the image processing in the real-time (frame rate minimally from 5 to 10 frames per second, ideally from 25 to 50 fps).

Our development started initially on a department of Military Academy in Brno (since 2004 University of Defence) in the year 2001 in cooperation with the firm OPROX, a.s., Brno. The centre of the work was gradually transferred into OPROX that has practically been the pivotal solver since 2006 (see the subsection 3.2).

The patents of POERF components have been published since the end of 1950's but there are no relevant publications dealing with the appropriate research and development results. We have not found out that similar device development is being carried out somewhere else. We have found only one agency information that a POERF was developed in Iran (www.ariairan.com, date: 20.7.2008). The problem itself consists particularly in users' unshakable faith in limitless possibilities of laser rangefinders and probably in the industrial/trade/national security directions (see the section 2).

Similar principle is applied to focusing system of some cameras as well as mobile robots navigation/odometry systems. Measured distance range is within order one up to tens of meters, therefore the hardware and software concepts in these systems are different from concepts in the POERF system. Sufficient literature sources cover these problems.

1.5 Future research

At present we have started the new period (2009 – 2012), in which we intend to fully handle the measurement of the target coordinates (for stationary and moving target) inclusive of the target trajectory extrapolation by POERF that can be set *on a moving platform*.

This work is supported by the Ministry of Industry and Trade of the Czech Republic – project code FR – TI 1/195: "Research and development of technologies for intelligent optical tracking systems". Also this chapter has originated under the support of financial means from this project.

2. Target Range Measurement System and the problem of fleeting targets

The accuracy of the target range measurement depends not only on properties of the rangefinder itself, but also on the whole system composed of the rangefinder, the atmosphere, a target, a target's surroundings, an operator and lighting – Fig. 3. Dependability and accuracy of the range measurement is characterized especially by the use of

- the probability of successful measurement of "whatever" range p_M (estimated by the relative frequency),
- the (sample) mean of measured range D_{T0} (resp. D_{Taver}),
- the (sample) standard deviation of measured range σ_D (resp. s_{TM}),
- the (sample) relative standard deviation of measured range $\sigma_{DR} = \sigma_D / D_{T0}$ (resp. $s_{DR} = s_{TM} / D_{Taver}$) and
- the probability p_D of the right (real) target range measurement, i.e. a range from the interval $\langle D_{T0} - \Delta D, D_{T0} + \Delta D \rangle$, where ΔD is chosen in compliance with the concrete situation, e.g. 10 m or 50 m.

Instead of the (sample) standard deviations σ (resp. s), corresponding probable errors E (resp. e) are often used. It is valid for normal distribution

$$E \approx 0.6745 \cdot \sigma . \quad (1)$$

The value of the relative probable error E is usually required less than 2 to 4% in a requisite interval of ranges under good conditions – daylight and meteorological visibility s_M (or MOR – meteorological optical range) over 10 km. This error is regarded as the error of appropriate Target Range Measurement System (TRMS), because the same error for measurement by the means of customary stadia methods (en.wikipedia.org/.../stadia_metric_rangefinding – targeting reticle) is usually 7 to 15% (in dependence on the operator training and tiredness; it is valid under nocturnal conditions, too).

In the case of pulsed laser rangefinders (LRF), the value $\Delta D = 5, 10$ or 15 m is frequently adduced as the indicator of their accuracy and, due to *advertising reasons*, it evokes the notion, that the probability p_D is almost 100% for the appropriate range interval and that is valid also for LRF maximal working range, e.g. 8 or even 20 km, and that it is the characteristic of the whole TRMS. We will explain shortly, what the reality is.

The precondition for range measurement by means of LRF (it is valid similarly for all active rangefinders – also radars, sonars) is the target irradiance by emitted laser beam – Fig. 4. The contractual target point T always lies on the beam axis. The usual divergence 2ω of LRF beam is from 0.5 to 1 mrad and for eyesafe LRF (ELRF) is lesser – circa to 0.3 mrad. In the case of fleeting target (the target is appearing surprisingly on shot time periods), it is

extremely difficult – or quite impossible – to aim at such target accurately enough and to realize the measurement. In the frequent case of relatively small target (e.g. a distant one), a very small part of the beam cross-section area falls to the target and the rest falls on the target surroundings – Fig. 4, 5. So, an estimate of surroundings range D_{N0} is usually measured, but the system is not able to distinguish it. This range is then presented as the estimate of the target range D_{T0} . It is a gross error of measurement. LRFs are equipped with a certain cleverness that allows helping in the gross error detection. Operator's experience is its fundamental. Nevertheless, these systems fail practically in the case of fleeting targets.

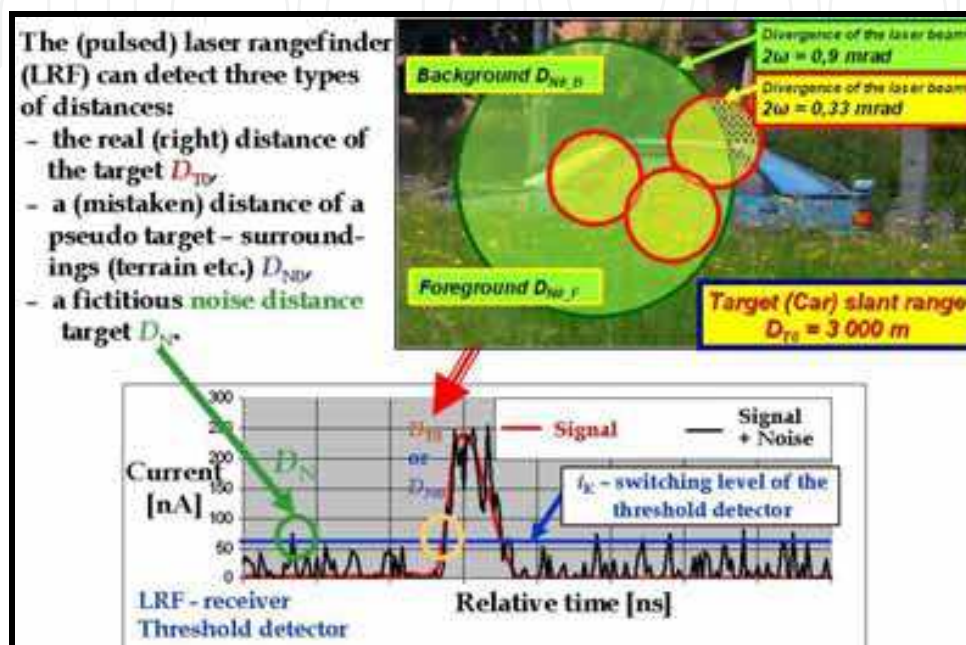


Fig. 4. Principle of influence of the laser beam divergence on the occurrence of gross errors in the target range measurement; more closely in (Apotheloz et al., 1981; Cech et al., 2006)

As clarified above, the aiming accuracy is decreasing in the cases of a fleeting target and an increase of tiredness and nervousness of the operator. The aiming accuracy will be characterized by the standard deviations in elevation σ_φ and in traverse (line) σ_ψ . We will assume a circular dispersion and hence $\sigma_A = \sigma_\varphi = \sigma_\psi$ is the (circular) standard deviation of ELRF. The example in the Figure 5 is from (Cech & Jevicky, 2005). It follows evidently, that the probability p_D of the right target range measurement depends significantly on the meteorological visibility and on the aiming accuracy.

The decrease of p_D under increasing range corresponds with the increase of the relative standard deviation σ_{DR} , and it is substantially greater than 5 or 10 m, as it can be incorrectly deduced from advertising materials.

However, it generally holds that the use of ELRF with the divergence of laser beam $2\omega < 0.5$ mrad requires the utilization of systems for aiming and tracking the target with extreme accuracy of the level $\sigma_\varphi \approx \sigma_\psi \approx \sigma_A \leq (0.1 \text{ to } 0.2)$ mrad.

Mentioned problems can be overcome by the use of POERF, which is able to work in both modes – online and offline. It is sufficient for measuring the target range that the target is displayed in fields of view of both cameras (sighting and metering), whereas their angles of view are in compliance with the system determination from 1.5° to 6° and therefore relative large aiming errors are acceptable.

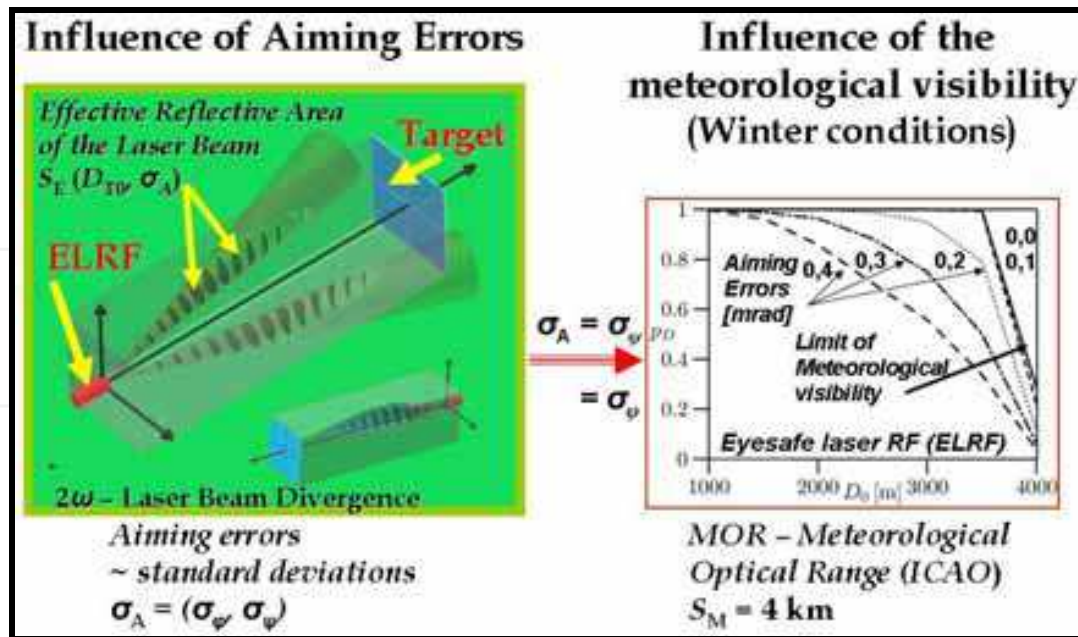


Fig. 5. Simulation experiment outputs – example (Cech & Jevicky, 2005): target 2.3×2.3 m and reflectance $\rho(\lambda) = 0.1$ for $\lambda = 1.54 \mu\text{m}$; $2\omega = 0.33$ mrad; $\Delta D = 5$ m

3. Short overview of the optical rangefinders evolution

3.1 General development of optical rangefinders

We will only deal with a subset of optical rangefinders (see en.wikipedia.org/.../Range_imaging), especially those ones which are based on measuring of parameters of the telemetric triangle lying in the triangulation plane and on consequential computation of estimate of the target slant range D_T . It is a special task solved within the frame of photogrammetry – more details in (Kraus, 2000), (Hanzl & Sukup).

These rangefinders are usually divided into three main groups: with the base in the ground space, with the base in the device (inner base) and with the base in the target.

Henceforth, we will not deal with rangefinders with the base in the target – see more details in (en.wikipedia.org/.../stadimeter).

The oldest system is an optical range-finding system with the base in ground space – Fig. 6. Ever since antiquity two “theodolites” placed at ends of the base have been used. It is possible to use only one theodolite which is transferred between ends of the base. A short history of theodolite development can be found in (Wallis, 2005).

Special theodolites (photogrammetric tracking theodolites) were progressively developed for measuring immediate positions of moving targets. They can be divided into two groups: without and with continuous recording of measurement results. Theodolites without continuous recording of measurement results were used for measuring positions of ships (en.wikipedia.org/.../Base_end_station), balloons and airplanes (Curti, 1945).

Theodolites with continuous recording of measurement results were used since 1930s for measuring positions of balloons (e.g. Askania Recording Balloon Theodolite – pibal theodolite), airplanes (en.wikipedia.org/.../Askania; e.g. Askania Cinetheodolite – kine-theodolite), (Curti, 1945) and projectiles (Hännert, 1928; Curti, 1945). The basis of these kine-theodolites was a special movie-picture camera. In connection with measuring positions of flying projectiles the term ballistic photogrammetry is used. Besides theodolites with

photographic registration, the ballistic cameras have been used for measuring positions of flying projectiles since 1900s (Hännert, 1928; Curti, 1945), e.g. Wild BC2 Ballistic Camera (since 1938), whose basis is a still camera modified for multiple repeated exposition of the projectile position on the same photographic plate.

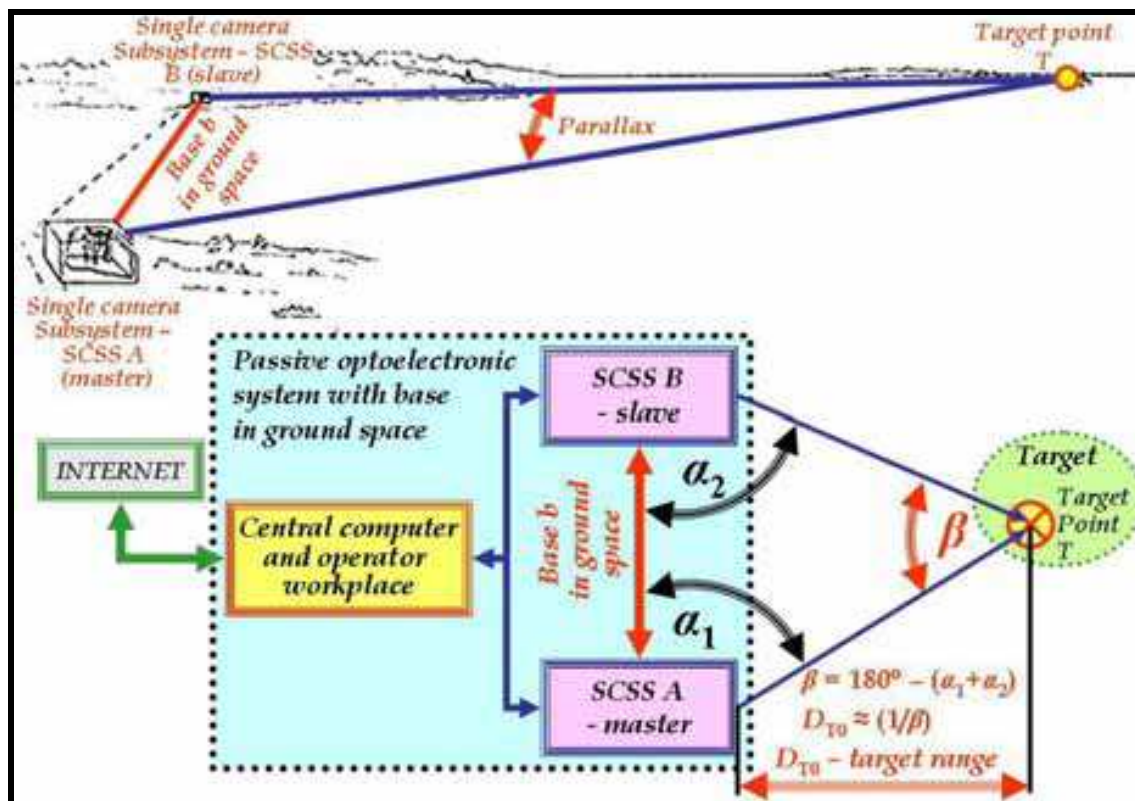


Fig. 6. Principle of the Optical Ranging System with the base in ground space

The next developmental step since 1940s (reference resources are not for disposal) could have been the usage of theodolites with cameras with video camera tube (pickup tube) (en.wikipedia.org/.../Video_camera), which have already made possible the picture watching on CRT monitor. Since 1956 there has been a possibility to record the picture on a video tape recorder – VTR (en.wikipedia.org/.../Video_recorder).

Our task (see the subsection 1.5) is the development of a single camera subsystem – Fig. 6 – with the usage of digital camera and Tit and Pan Device (System, Assembly).

Optical rangefinders with the base in the device are divided into coincidence and stereoscopic rangefinders. The production of both types started already in 1890s. The first coincidence rangefinders were made by Scottish firm Barr and Stroud (Russall, 2001). The first stereoscopic rangefinders were made by German firm Zeiss. Theory, projection and adjustment are published in (Kepert, 1966). The construction principles and utilization of these rangefinders can be found in (Composite authors, 1958; Curti, 1945). One of the first constructions of POERF is described in (Gebel, 1966). It is a modification of a coincidence rangefinder with the utilization of one piece of a special pick-up transducer tube (U.S. Patent 2 969 477, author Gebel, R. K. H.). U.S. Patent presupposing utilization of two television sensors (Gilligan, 1990), which is a modification of stereoscopic rangefinder, adverts to older patents, whereas the oldest patent is U.S. Patent 2 786 096 Television rangefinder (Palmer, march 1957). Subsequent patent applications of POERF presuppose the

usage of linear array CCD sensors, for instance the application No. PCT/AU1990/000423 Passive-Optoelectronic Ranging. Patent applications presupposing the use of digital matrix sensors (CCD or CMOS) have not been found till now.

The first commercially offered CCD sensor (100 × 100 pixels) was produced by the firm Fairchild Imaging in the year 1973. The first really digital cameras did not originate until the half of 1980s. The serial cameras with resolution e.g. 640 × 480 pixels were not offered until the half of 1990s.

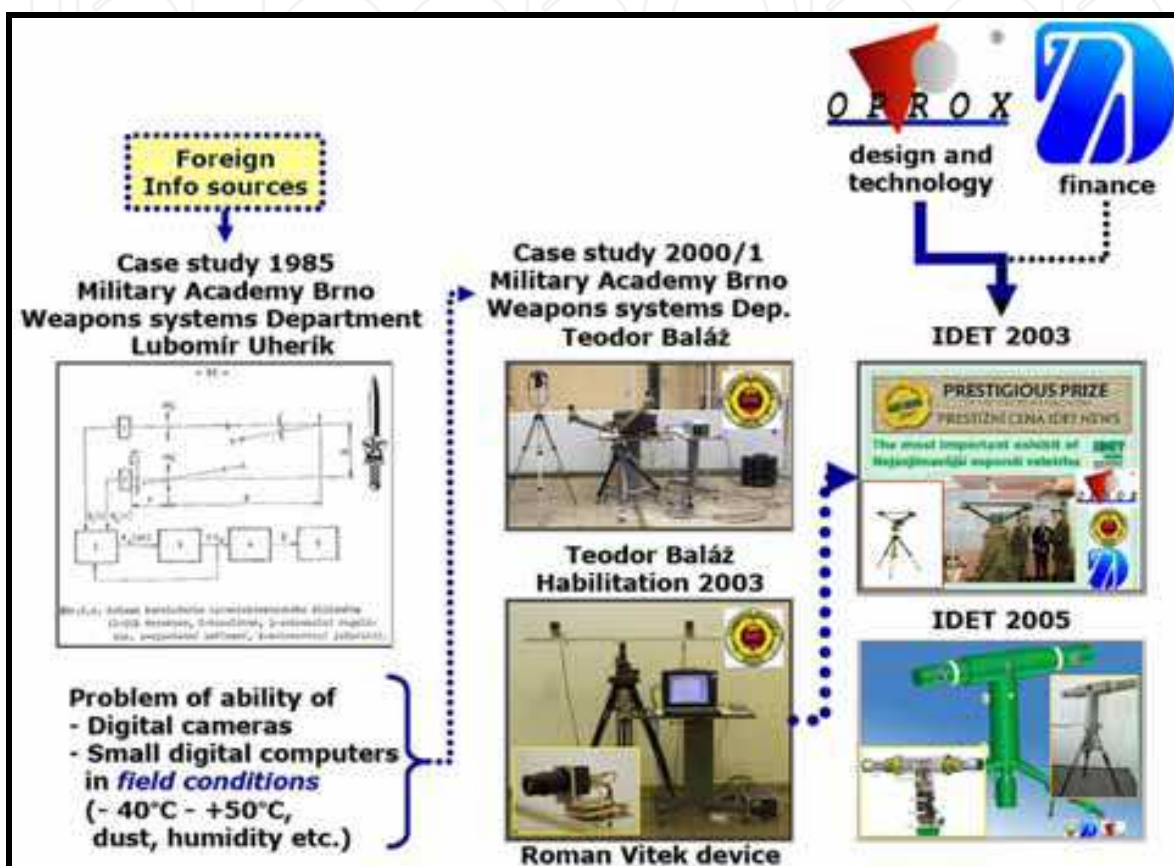


Fig. 7. Brief summary about the research and development of POERF in the Czech Republic

If we observe the development of sufficiently small and efficient computers whose construction is resistant to environmental influences, we find out that they appeared in the market as lately as the second half of 1990s.

According to the article (Jarvis, 1983), one of the oldest algorithms for stereoscopic disparity finding from which the estimate of the target range is computed – the cross-correlation algorithm – was already published e.g. in (Levine et al., 1973). The fundamental classification and comparison of algorithms for finding of stereoscopic disparity can be found for instance in (Scharstein & Szelisky, 2002). The date of this publication corresponds to the period when the basic hardware means (cameras and computers) have begun to satisfy requirements for the construction of components for fully digital POERF.

3.2 POERF development in the Czech Republic

The development of the passive optoelectronic rangefinder has proceeded in the Department of Weapon Systems of the Military Academy in Brno (since the year 2005 the

Department of Weapons and Ammunition of the University of Defence) and in firms cooperating with the department, especially in the firm Oprox, a.s.

Based on the study of foreign sources, the fundamental properties of POERF were analyzed in the study (Uherik et al, 1985) – Fig. 7. The research and development of POERF started as late as the year 2001 after accomplishment of the objective properties.

The development can be divided into three periods as it is shown in the Figures 7 and 8.

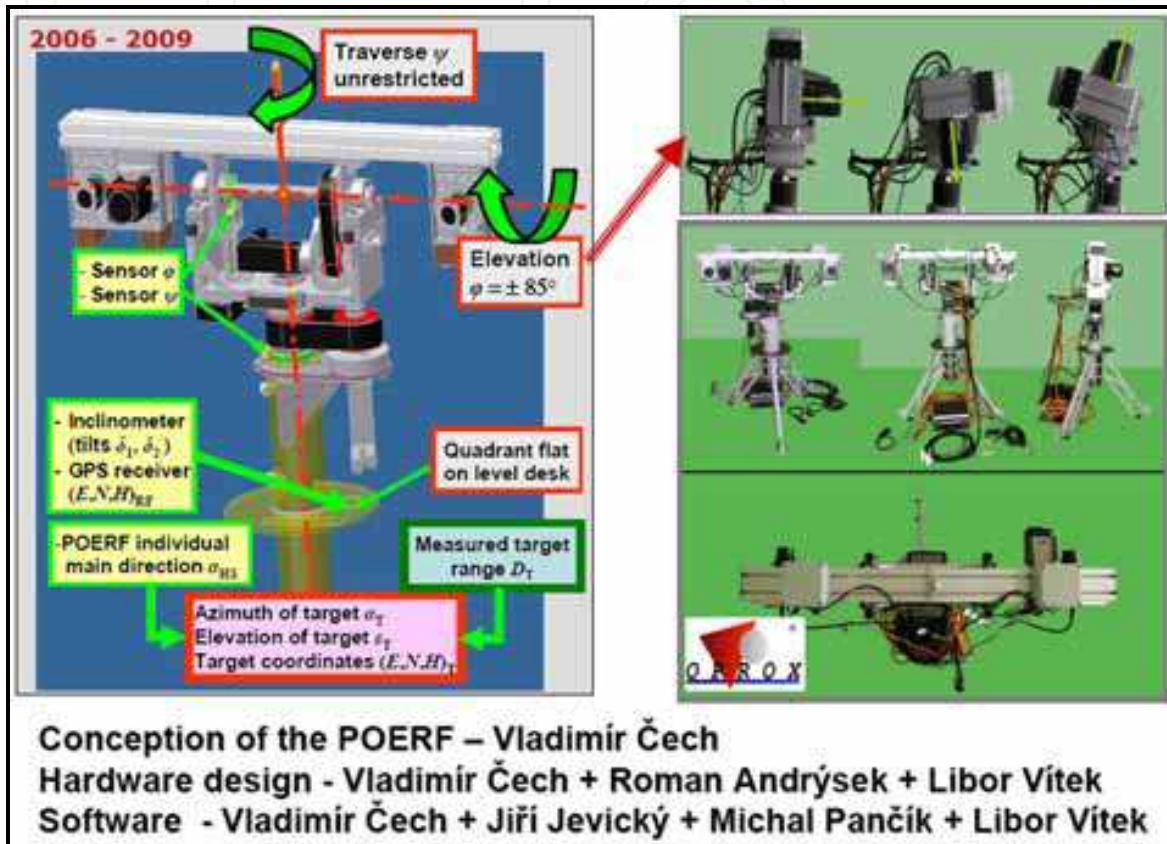


Fig. 8. The third demonstration model of POERF from the year 2009; the project manager was Jozef Skvarek

In the first period (2001 to 2003), the basic principles were verified (Balaz, 2003). The first demonstration model of POERF was awarded in the 7th International Exhibition of Defence and Security Technologies and Special Information Systems in Brno (IDET 2003). The development was supported during a certain period by the firm Z.L.D., s.r.o., Praha.

In the second period (2003 to 2006), the technology of the range measurement of a stationary target was handled (Skvarek, 2004). The second demonstration model was developed and introduced at the exhibition IDET 2005. Authors of this chapter have joined in the research and development of POERF in the year 2003.

In the third period (2006 to 2009), the measurement of coordinates of a moving target and its trajectory extrapolation (Cech et al., 2009a) belonged among main extensions of POERF functionality. Starting this period, the crux of the work was transferred into the firm Oprox, a.s. The third demonstration model was the final result of the research and development in this period – Fig. 8.

At present we have started the fourth period (see the subsection 1.5).

4. POERF – demonstration model 2009

From the system view, the POERF as a mechatronic system is composed of three main subsystems, Fig. 1, 8 (Cech & Jevicky & Pancik, 2009d):

- the range channel,
- the direction channel and
- the system for evaluation of the target coordinates and for their extrapolation.

The task of the range channel is on the one hand automatic recognition and tracking of the target which has been selected by the operator in semiautomatic regime and continuous measuring of its slant range D_T (c. 10 measurements per second at present, which is identical to cameras frame rate) and on the other hand the evaluation of angle measured errors (e_φ, e_ψ) that are transferred to input of the direction channel – Fig. 12.

The direction channel – its core consists respectively of two servomechanisms and of special Pan and Tilt System (Device, Assembly) – ensures continuous tracking of the target in the automatic and semiautomatic regime and measuring of angle coordinates of the target (the elevation φ and the traverse ψ) – Fig. 1, 8. The elevation range is c. $\pm 85^\circ$ and the traverse potential range is not limited – Fig. 8. The real range of the traverse is limited to c. $\pm 165^\circ$ by two terminal sensors due to safeguard protection of cables – Fig. 8. The optical sensors SIGNUM™ RESM 20 μm by the firm RENISHAW® are used for the detection of elevation and traverse. The spherical coordinates of the target (D_T, φ, ψ) are transformed into the UTM coordinates by the system for evaluation of the target coordinates and their extrapolation – Fig. 1, 2, 15. Withal, the knowledge of the POERF geographic coordinates (E, N, H)_{RF} and the POERF individual main direction a_{HS} (Fig. 8) is utilized. In the case of moving target, required extrapolative parameters are consecutively evaluated (coordinates of the measurement midpoint, corresponding time moment and the velocity vector of the target). The extrapolative parameters (UTM coordinates of the target are transformed into geographic coordinates WGS 84) are sent periodically to a user in near-real-time (at the present with the period 1 second, i.e. the data “obsolescence” is c. 0.5 seconds) – Fig. 2, 15.

POERF must be adjusted so that the traverse axis is vertical. Due to this, the setscrews are situated in the bottom ends of the support legs – Fig. 8. The main tool for the adjustment is the level or the quadrant which can be placed on the quadrant flats on the level desk. Two inclinometers placed perpendicularly to each other will be used in the future – Fig. 8.

The demonstration model 2009 works only in the online mode.

4.1 Range channel

As mentioned above, the main task of the range channel is on the one hand automatic tracking of the target which has been selected by the operator in semiautomatic regime and continuous measuring of its slant range D_T and on the other hand the evaluation of angle measured errors that are transferred to the input of the direction channel.

The core of hardware consists of three digital cameras fixed through adjustable suspensions to the cameras beam – Fig. 1, 8, 9. The camera of type Basler A101p (image size 2/3”; C Mount; monochromatic CCD sensor SONY IXL085AL with 256 brightness levels, the number of columns is $n = 1\,300$, $c = 1, 2, \dots, n$; the number of rows is $m = 1\,030$, $r = 1, 2, \dots, m$; square pixels $\rho(c) = \rho(r) = \rho = 6.7 \mu\text{m}$) was chosen for the sighting and metering cameras. The type IQ 753 by the firm IQinvision (image size 1/2”; CS Mount; the number of columns is $n = 2048$, the number of rows is $m = 1536$, square pixels $\rho(c)$

$= \rho(r) = \rho = 3.1 \mu\text{m}$, exploited 256 monochromatic brightness levels) was used as the spotting camera.

The algorithm for computation of estimate of a slant range D_T is based on solution of the telemetric triangle that lies in the triangulation plane - Fig. 9, 10. The input data are ordinal numbers c_{T1} , c_{T2} of columns of matrix sensors in which images T'_1 , T'_2 of the target point T are projected. In particular, it is sufficient to determine their difference Δ_{CT} (horizontal stereoscopic disparity) that is proportional to the appropriate parallax angle β . Therefore algorithms for computation of estimate of the difference Δ_{CT} are crucial (the correspondence problem algorithms). We work with algorithms for an estimate of Δ_{CT} , which involve the definition of 2D model of the target image (shortly "target model"). We use a rectangular target model for the present (Marik et al., 2003). This size (in pixels: rows \times columns = $(2m_M + 1) \times (2n_M + 1)$) is adjustable (the default setting is 51×51 pixels) - Fig. 12. Apex of the main aiming mark lies always in the centre of the target model - Fig. 12. The contour of the target model is not displayed in the image from the sighting camera - Fig. 13.

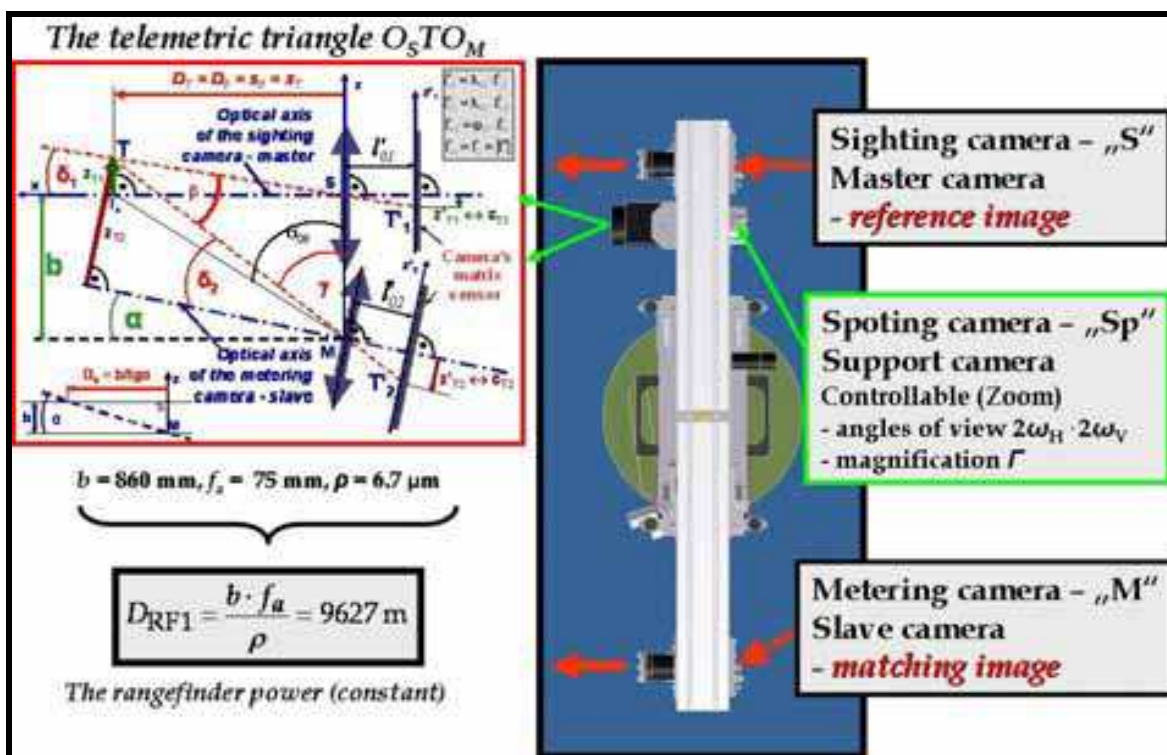


Fig. 9. Basic arrangement of the range channel hardware

The positive value $d_T = C_{ORF} - \Delta_{CT}$ is usually regarded as the disparity. The sign convention is elected so that $\Delta_{CT} \geq 0$ is valid for $D_T \geq D_a$ - Fig. 9, 10, where $D_a = b / \tan a$. The size of the convergence angle a (resp. a) - Fig. 9, 10 - is chosen with respect to the requirement that the measurement of the given minimal range D_{Tmin} of the target should be ensured. In our case $D_a = c. 50 \text{ m}$. The columns $c_{20} \approx c_{10} \approx 1300/2 = 650$ determine the horizontal position of the principal points of autocollimation/projection. If the target is in infinity (the Sun, the Moon, stars), then its disparity is just $\Delta_{CT} = C_{ORF}$. The rated value $C_{ORF} = 190.317$ pixels - Fig. 10.

The rangefinder power (constant) D_{RF1} is the basic characteristics of potential POERF accuracy - Fig. 10, 11. With increasing value of the power, the accuracy of measurement increases too. The power of POERF demonstration model is $D_{RF1} = 9627 \text{ m}$ - Fig. 9, 10. The

size of D_{RF1} depends on the width of rows of pixels $\rho(c)$, on the absolute value of the image focal length f_a and on the size of the base b .

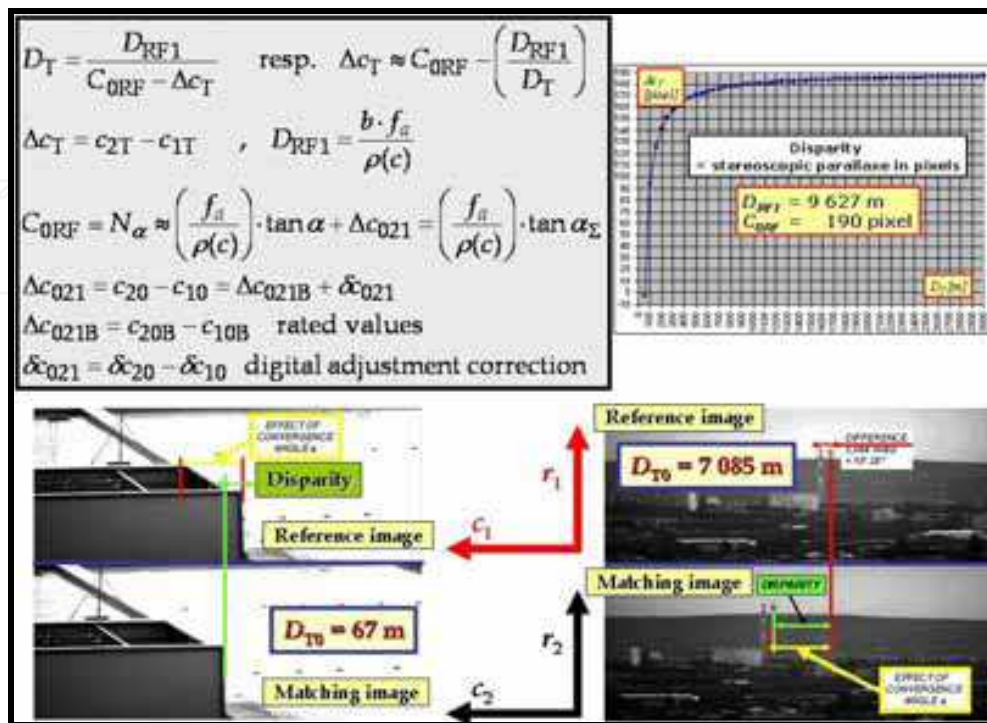


Fig. 10. The main relations for computation of the estimate of the target slant range D_T from the estimate of the horizontal disparity Δc_T (the coordinates $(r, c)_i, i = 1, 2$ are coordinates of the digital matrix sensors of the sighting and metering cameras)

The choice of the size $\rho(c)$ (resp. ρ) is a compromise between the effort to achieve the maximum potential well depth, which is increasing with the size of ρ , and the minimal image size of the sensor, whereas many other demands on the camera parameters must be reflected. The choice of size of the (absolute value) image focal length f_a results from the requirement that the sorted type of the target (e.g. passenger vehicle) must be identifiable in the requisite maximum spotting range $D_{T_spot_max}$ of the rangefinder ($D_{T_spot_max} \geq D_{Tmax}$ - the maximum working range). In accordance with Johnson criterion (50% successfulness of the target identification under excellent meteorological visibility $s_M \geq 10 \text{ km}$), the target has to be displayed minimally on 16 times 16 pixels (Holst, 2000), (Balaz et al., 1999). In practice, the resolution of the target image should be minimally 32 times 32 pixels (Cech et al., 2009).

The real maximum spotting range of the sorted target type $D_{T_spot_max}$ depends simultaneously on the up-to-date horizontal meteorological visibility s_M . The final choice of the value f_a is influenced by the demands imposed on the lens. It affects chiefly the size of angles of view and these angles determine potential possibilities of POERF in the offline mode (see the section 2). For example, it is valid for the horizontal angle of view

$$2\omega_H = 2 \cdot \arctan \left(\frac{n \cdot \rho(c)}{2 \cdot f_a} \right). \tag{2}$$

It is evident from this relation that it is advantageous to use the camera with sensor with a large number of columns n . The lenses PENTAX B7518E (1" format Auto-Iris DC, C Mount;

$f_a = 75$ mm, the minimal aperture ratio $a_{\min} = 1.8$) have been chosen for the sighting and metering cameras. Their horizontal angle of view is 6.65° and vertical 5.27° . The lens PENTAX H15ZAME-P with the zoom 1 to $15\times$ ($1/2''$ format Auto-Iris DC; C Mount; $15\times$ Motorized zoom - DC, $f_a = 8$ to 120 mm, minimal aperture ratio $a_{\min} = 1.6$ (resp. 2.4)) has been chosen for the spotting camera.

The last parameter that influences the size D_{RF1} is the length of the base b . Its size is selected with respect to the demand for accomplishment of requisite size $D_{T0} = D_{T\max}$ - the maximum working range, in which the relative size of the probable error E_{DR} of the range measurement attains the given size, e.g. 3% - Fig. 11. The size of the base b depends simultaneously on the size of the standard deviation $\sigma(c)$ (resp. σ_C) of determination of the disparity Δ_C corresponding to the range $D_{T\max}$.

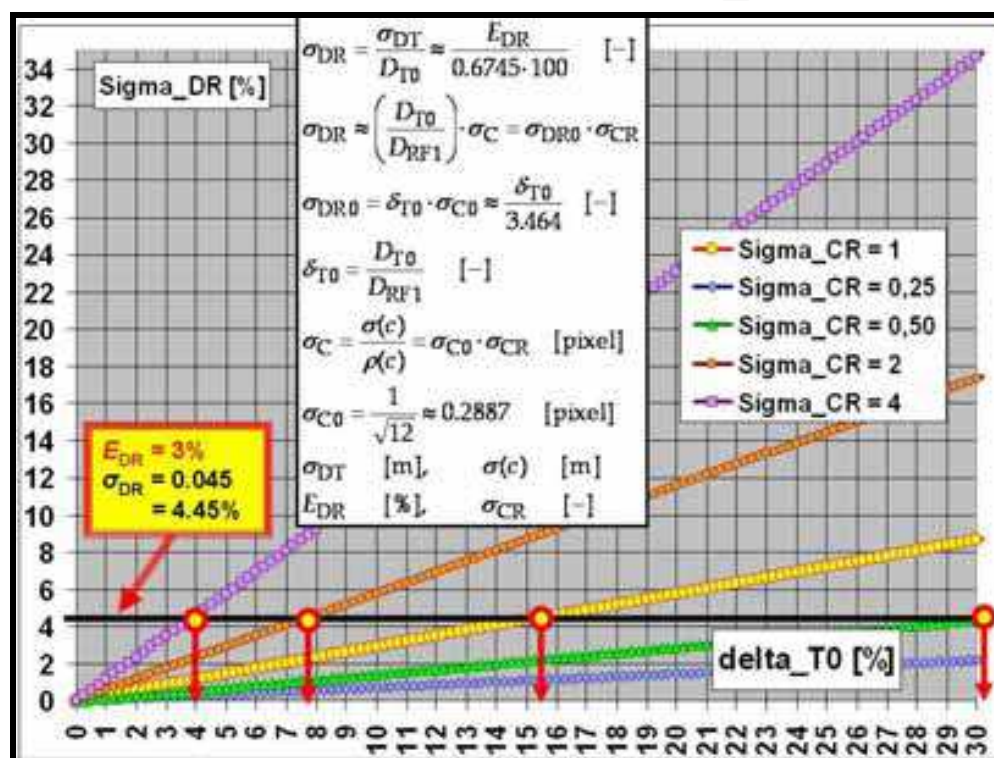


Fig. 11. The main relations for estimate of POERF accuracy

As its basic (standardizing) value σ_{C0} can be elected the standard deviation that originates always in finding the *integer* value of the disparity Δ_C as an unrecoverable discretization (quantizing) noise with the uniform distribution on the interval of the length just one pixel. Then it is $\sigma_{C0} \approx 0.2887$ - Fig. 11. Instead of values σ_C , their relative values σ_{CR} can be used as well. The value σ_C (resp. σ_{CR}) is the quality indicator for appropriate hardware and software of the POERF, especially for algorithms for estimates of sizes of the disparity Δ_C under given conditions (meteorological visibility, atmospheric turbulence, exposure time, aperture ratio, motion blur, etc.). If the value of σ_{CR} increases twice, then it is necessary to elongate the base b also twice with a view to preserve the requisite value $D_{T\max}$. Whence it follows that the quality of hardware and software immediately influences the POERF sizes that are directly proportional to the size of base b . The used base is 860 mm long.

The actual values of constants D_{RF1} and C_{ORF} are determined during manufacturing and consecutively during operational adjustments. The adjustment is realized under utilization

of several targets whose coordinates are known for high accuracy. The appropriate measurements are processed statistically with the use of the linear regress model (the component part of POERF software – Fig. 14). For example, it was determined for targets 1 to 33 from the Catalogue of Targets (see the section 5, the Figures 16, 17) and for integer estimates of the disparities that $D_{RF1} = 9\,215.5$ m and $C_{ORF} = 195.767$ pixels (the correlation coefficient $r = -0.999\,725$).

The starting situation in the process of a target searching and tracking can be characterized as follows. The operator has only common information that a potentially interesting object (the future target) could be in a given area. In the first period, the operator (sometimes with the help of other persons) usually searches an odd object in the area under interest with his eyes only or with the use of tools, e.g. field-glasses, and also with the help of POERF that works in the regime “searching” in which the angles of view of the spotting camera are sufficiently large (ideally c. 40° to 50°).

As soon as the target is identified and localized, the first period is closed and the second period starts. The operator creates the first estimate of model of the target on the monitor from the image provided by sighting camera (master) and passes on the computer. Sizes of the first estimate of the target model must be sufficiently large – under aiming errors that correspond to the actual situation and that are characterized by standard deviations in the elevation σ_φ and in the traverse σ_ψ – because the operator needs to place the real target into the area of model of the target reliably – Fig. 12. Whenever he thinks that he attains it in the process of sighting and tracking of the target, he pushes the appropriate button (Fig. 13) and thus he passes the target model to the use in algorithms of automatic tracking of the target and measuring of its range.

In the third period, the target position and its range are evaluated automatically. The operator tries to reduce sizes of the target model (the POERF demonstration model 2009 does not enable it) and to place it again on the target. In the case of success, he pushes the appropriate button and the system starts the exploitation of a new target model. The whole process is supported by automatic stabilization of positions of optical axes of cameras and eventually also by additional stabilization of the image on operator’s monitor (it is not implemented in the demonstration model 2009). The operator can terminate this process as soon as the target model includes pixels with only a part of image of the real target. Complications are caused by objects which are situated in front of the target and are badly visible, e.g. branches of bushes and trees, the grass, but also raised dust. The operator consequently monitors automatically proceeding process. He enters into it in the case of disappearance of the target behind a barrier for a longer time. In the case that information about extrapolated future position of the target is exploited, a short disappearance of the target can be compensated by the automatic system (not implemented in the demonstration model 2009). The level of algorithm ability to learn will determine if the operator’s intervention is needful in the case of the target turning to markedly other position towards the POERF.

The program for automatic tracking of a target is based on the utilization of procedures from the library Open CV, specifically on a modification of Lucas Kanade algorithm (Bouguet, 1999). If the target disappears momentarily behind a barrier, then the algorithm collapses. The operator must intervene as it is explained above.

The program starts its functions as soon as the operator pushes the button “Start Measurement” or “Start Tracking”. The algorithm then finds the nearest corner (of an object) to the apex of the main aiming mark in the shot from the sighting camera. This point is

considered the image T_1 of the target point T but only due to needs of the target tracking – Fig. 9. Consequently, just two last consecutive shots from the sighting camera are processed. With utilization of Lucas – Kanade Feature Tracker algorithm (Bouguet, 1999) for evaluation of the optical flow, the position of the corner – the point T_1 – is always estimated in the consequent shot with a subpixel accuracy. The algorithm is robust and that is why it can cope with a gradual spatial slew of the target. The algorithm simultaneously highlights in the image on the monitor the points, which have been identified as appurtenant to the moving target, so that the operator has in his hands the screening control over the system activity. In the case of problems, it is necessary to use 2D model of the target as mentioned above. The point T_1 is at the same time considered the aiming point T_{AP} – Fig. 12, and so the control deviations (e_φ, e_ψ) are evaluated (as measured errors of angles) for the direction channel control – Fig. 12.

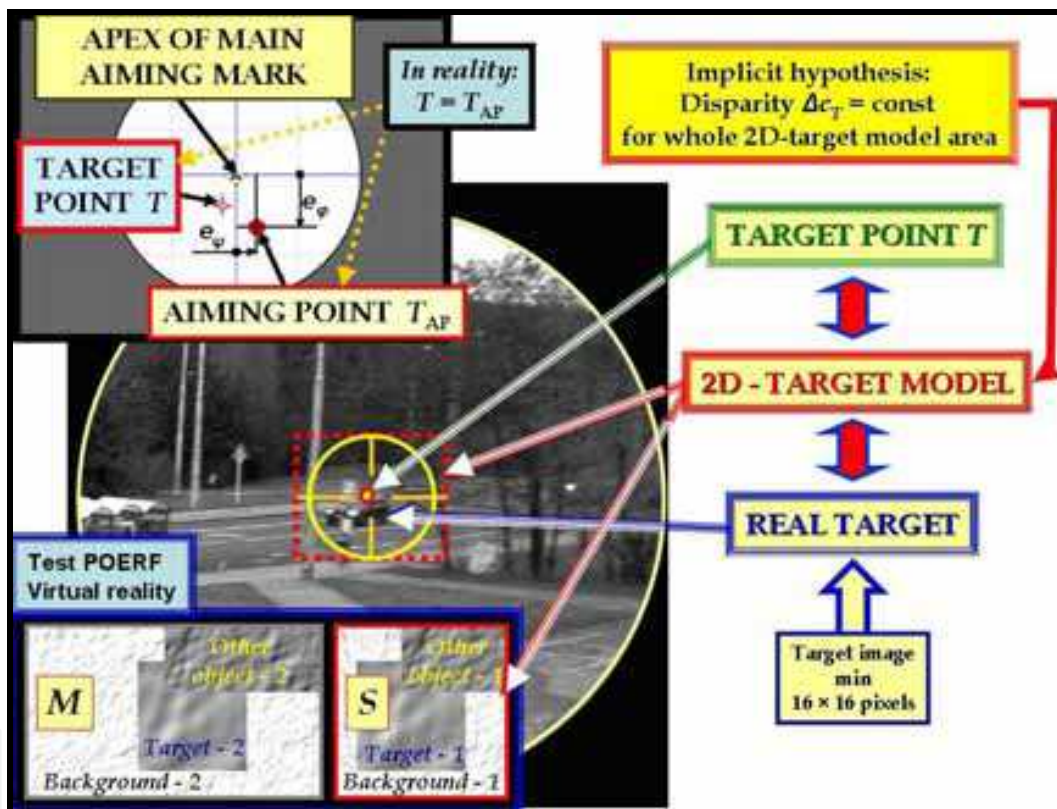


Fig. 12. Relation among the image of the real target in the sighting camera, the target point T and 2D model of the target

The maximum computing speed is required primarily, in order that about 30 range measurements per second are necessary in our applications (POERF). Therefore, we prefer simple (and hence very fast) algorithms. Random errors of measurements are compensated during statistical treatment of measurement results (extrapolation process).

The matching cost function $S(k)$ is used in the meantime (in general it is pixel-based matching costs function) – the sum of squared intensity differences SSD (or mean-squared error MSE) (Scharstein & Szelisky, 2002). The computation of matching cost function $S(k)$ proceeds in two steps.

Firstly, its global minimum with one-pixel accuracy is calculated (the tabulation over all admissible horizontal shifts of the 2D target model on the matching image). Simultaneously,

the constriction for the choice of the global minimum – known as the Range Gate (Cech et al., 2009) – is applied.

In the second step, the global minimum is searched with sub-pixel accuracy while using the polynomial approximation (the interpolation and the least-squares method can be alternatively used) in the neighbourhood of the integer point of the global minimum, which has been found in the first step.



Fig. 13. Five basic windows for the operator during the target spotting, aiming and in the beginning of the measurement or tracking

While using above-mentioned algorithms, it is always presumed that the same disparity $\Delta c_T = \text{const}$ is for all pixels of 2D target model – Fig. 12. This precondition is equivalent to the hypothesis that these pixels depict immediate neighbourhood of the target point T representing the target and this neighbourhood appertain to the target surface (more accurately all that is concerned the image T'_1 of this point and its neighbourhood). These algorithms belong to the group referred to as local, fixed window based methods.

Added precondition can be frequently satisfied by a suitable choice of size and location of the target model (i.e. by the aim of a convenient part of the target). The choice is performed iteratively by the operator for the real POERF.

Usual shapes of a target surface (e.g. balconies on a building facade, etc.) have only a little influence on the above-mentioned precondition violation, because the range difference generated by them is usually less than 1 to 2 percent of the “average” target slant range D_T evaluated over the target surface represented by the 2D target model.

Operations over the set of pixels of the 2D target model that generate the matching cost function $S(k)$ and the procedure of its minimum searching can be counted as a definition of special moving average, and – as a consequence – the whole process appears as a low-frequency filtration.

It holds generally that if respectively the meteorological visibility is low and the atmosphere turbulence is strong, then it is necessary to choose a larger size of the 2D target model, i.e. to filter out high spatial frequencies loaded by the largest errors and to work with lower spatial frequencies.

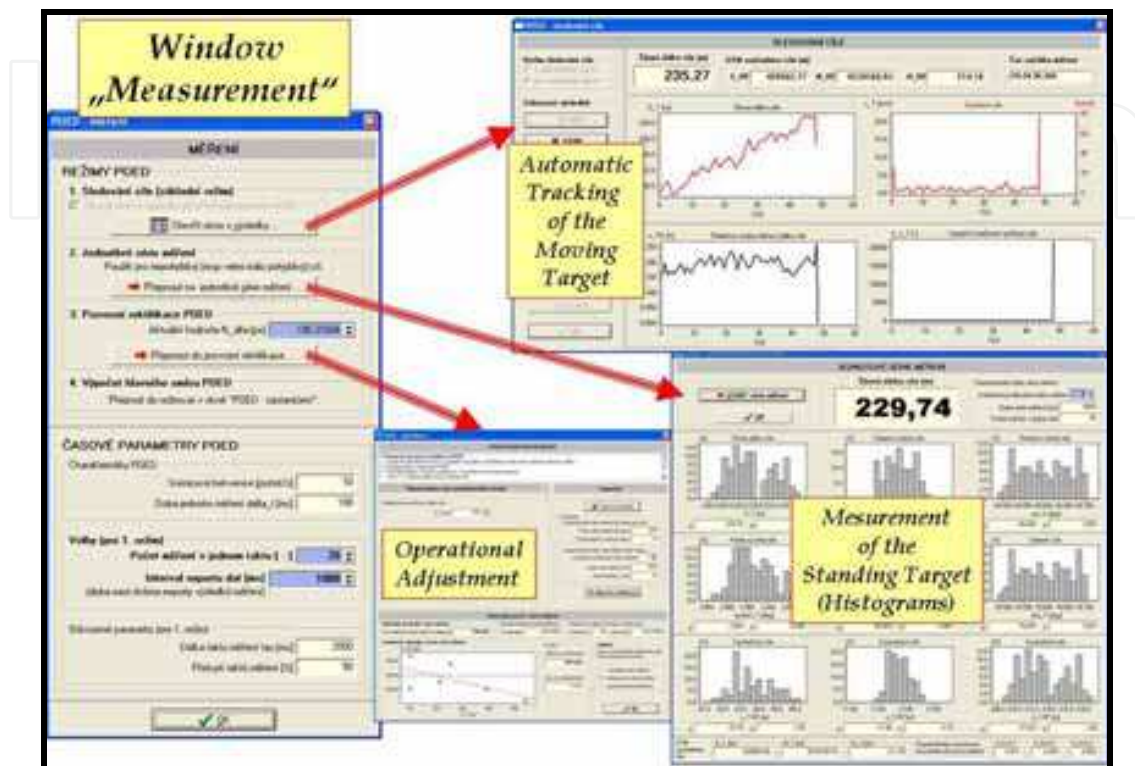


Fig. 14. Auxiliary windows for monitoring of respectively the measurement and the adjustment

In many cases it is inevitable that some pixels of the 2D target model record a rear object or a front object instead of the target – Fig. 12. Simulation experiments with the program Test POERF showed (Cech & Jevicky, 2007) that farther objects have minimal adverse impact on the accuracy of the range measurement, contrary to nearer objects that induce considerably large errors in the measurement of the target range. From the problem merits, these errors are random blunders. Their greatness depends on the mutual position of the front object and the target – Fig. 12. This finding has been also verified in computational experiments by the help of the program RAWdis (Cech & Jevicky, 2010b). It is a specific particular case of more common problem that is known as occluded areas; the specific case is the result of the depth discontinuity (Zitnick & Kanade, 2000).

It is evident from the above that the choice of the position and the size of 2D target model is not a trivial operation and it is convenient to entrust a man with this activity. The operator introduces a priori and a posteriori information into the measurement process of respectively the disparity and the range of a target and this information can be only hardly (or not at all) obtained by the use of fully automatic algorithm.

Algorithms commonly published for the stereo correspondence problem solving are altogether fully automatic – they use the information included in the given stereo pair images, eventually in several consecutive pairs (optical flow estimation). Therefore, it is possible to get inspired by these algorithms, but it is impossible to adopt them uncritically.

In conclusion it is necessary to state that these automatic algorithms are determined for solving the dense or sparse stereo-problems, whereas the algorithms for POERF estimate the disparity of the only point – the target point T , but under complicated and dynamically varying conditions in the near-real-time.

4.2 Direction channel

The purpose of the direction channel is already mentioned above.

The core of the direction channel (Cech et al., 2009a) comprises two independent servomechanisms for the elevation φ and the traverse ψ – Fig. 8. Identical servomotors and servo-amplifiers by the firm TGdrives, s.r.o., Brno were used there. AC permanent magnet synchronous motors (PMSM) TGH2-0050 (24 VDC) have a rated torque 0.49 Nm and a rated speed 3000 rpm. The servo-amplifiers are of the type TGA-24-9/20. Furthermore, cycloidal gearheads TWINSPIN TS – 60 from the firm Spinea, s.r.o., Presov with the reduction ratio respectively 47 (elevation) and 73 (traverse) were used. Reduction ratio of the belt drive is respectively 1.31 and 1.06.

The properties of the range channel and of the direction one are bound by the relation (Cech et al., 2009)

$$\theta = \Delta\omega \cdot \Delta t_{E_lag} \leq \theta_{max} = \frac{\delta c_{max} \cdot \rho(c)}{f_a}, \quad (3)$$

where

θ_{max} is the maximum permissible measurement error of the parallactic angle β – see the Figure 9,

δc_{max} is the same error expressed by pixels, e.g. $\delta c_{max} = 0.1$ (resp. 0.05) pixel,

Δt_{E_lag} is the absolute value of the time difference between starting the exposition in the sighting camera and in the metering one,

$\Delta\omega = |v_{Tp}/D_T - \omega_S|$ is the absolute value of the error of the immediate angular velocity in the elevation/ traverse,

\mathbf{v}_{Tp} is the appropriate vector component of the relative velocity of the target in the plane, which is perpendicular to the radius vector of the target (i.e. perpendicular to the vector determined by the points P_{RF} and T),

ω_S is the appropriate immediate angular velocity in the elevation/ traverse, which is generated by the servo-drives.

It is evident from the relation (3) that the primary attention should be paid to the exact time synchronization of expositions of the sighting camera and the metering one (resp. to the synchronous sampling of the all relevant data), and that the increase of demands on the precision of servo-drives is less important. It is interesting to retrace solutions of the problem in former times (en.wikipedia/.../Base_end_station).

4.3 Target trajectory prediction

Algorithms used in the demonstration model POERF have been evolved by authors of this chapter (Cech & Jevicky, 2009b). Consequently, they have created appropriate software. Firstly, they developed a tuning and test simulation program and secondly, they have programmed procedures for the library POED.DLL (these procedures are exploited by the control program of POERF).

Trigonometric calculations relate to points P_{RF} (coordinates $(E, N, H)_{RF}$) and T (coordinates $(E, N, H)_T$), but rangefinder and target are spatial objects with nonzero sizes. It arises the fundamental problem, how and where to set unique contractual point on the rangefinder, and analogously, how and where to set (preferably uniquely) contractual point on the area of target image in the sight.

Chosen position of the point T in the target image determines simultaneously its position in the space. This point T is conventionally described as the "target point", i.e. reference point that represents the target at given moment due to needs of measurement of the target position.

Rangefinder construction can require aiming by the sight not into the target point T , but into so-called "aiming point" T_{AP} . Its position must be chosen in accordance with instructions for the work with rangefinder. In our case, the aiming point T_{AP} is identical with the target point T – Fig. 12.

As a result of aiming errors (Fig. 12), the position of the apex of the main aiming mark in the rangefinder sight (that represents the position of sensitive axis of the rangefinder in the space) does not coincide with the position of the aiming point T_{AP} image in the sight at the moment of range measurement. It is usually the source of additional errors in measurement of the target position in the space because the range to the point T' is measured (and it is possible that this point lies off the target), but the range is interpreted as range to the target point T . In this case, a gross error appears in the target range measurement.

By reason of simple derivation of seeking dependencies, it is necessary to introduce several coordinate systems. Detailed analysis of this problem was already presented in (Cech et al., 2009a).

The measurement point (j -th point of measurement $T_j = T(t_j)$) denotes position of the target point T at the moment t_j that characterizes contractually the moment of taking the stereo-pair images, from which the target slant range D_{Tj} is evaluated.

Data record (j -th record) – means a process beginning by preparation for taking the stereo-pair images (time $t_{STARTj} = t_{sj}$) and ending (time $t_{STOPj} = t_{kj}$) by completion of export of evaluated estimate of the target coordinates (generally $(E, N, H)_{Tj}$), that are contractually related to the "measurement moment", i.e. in the time t_{STOPj} , the target coordinates are given to the next use for all system. The length of record continuance is $T_{Zj} = t_{STOPj} - t_{STARTj}$.

Observing period is the time interval between two consecutive records (exports of data – the target coordinates) $t_{OPj} = t_{kj} - t_{kj-1}$. This period is usually constant, $t_{OPj} = t_{OP} = \text{const}$.

On the basis of information from publications and supposed accuracy of the test device POERF, the linear hypothesis about target motion was selected (presumption of uniform straight-line motion of the target with constant speed) as the most robust hypothesis from applicable ones. This hypothesis, in the case of immovable target, degenerates automatically into hypothesis of stationary target. Measured data are smoothed by linear regress model. Application of Kalman filter is problematic enough, especially due to low frequency of the target slant range measurement. This frequency is c. 10 to 100 times lower than it is usual in radiolocation. Needful organization of all processes follows from adduced preconditions – Fig. 15.

Total N_k data records – measurements ($j = j_{\min k}, \dots, j_{\max k}$) are evaluated together in the k -th cycle. In our model there is $N_k = \text{const}$ for $k = 2, 3, \dots$ and $N_1 = N_2 \cdot P_{1,0}$. Linear regress model is applied on data from these records.

One measurement period Δt_{MES1} , as the interval between two successive measurement points, is estimated from the rate frame [fps]. Measurement cycles overlap $P_{k,k-1} = 1 -$

(N_{SHk}/N_k) is in functional relation with the interval of data export T_{SHk} . The overlap of measurement cycles denotes what relative number of records (measurements) is shared by two successive cycles.

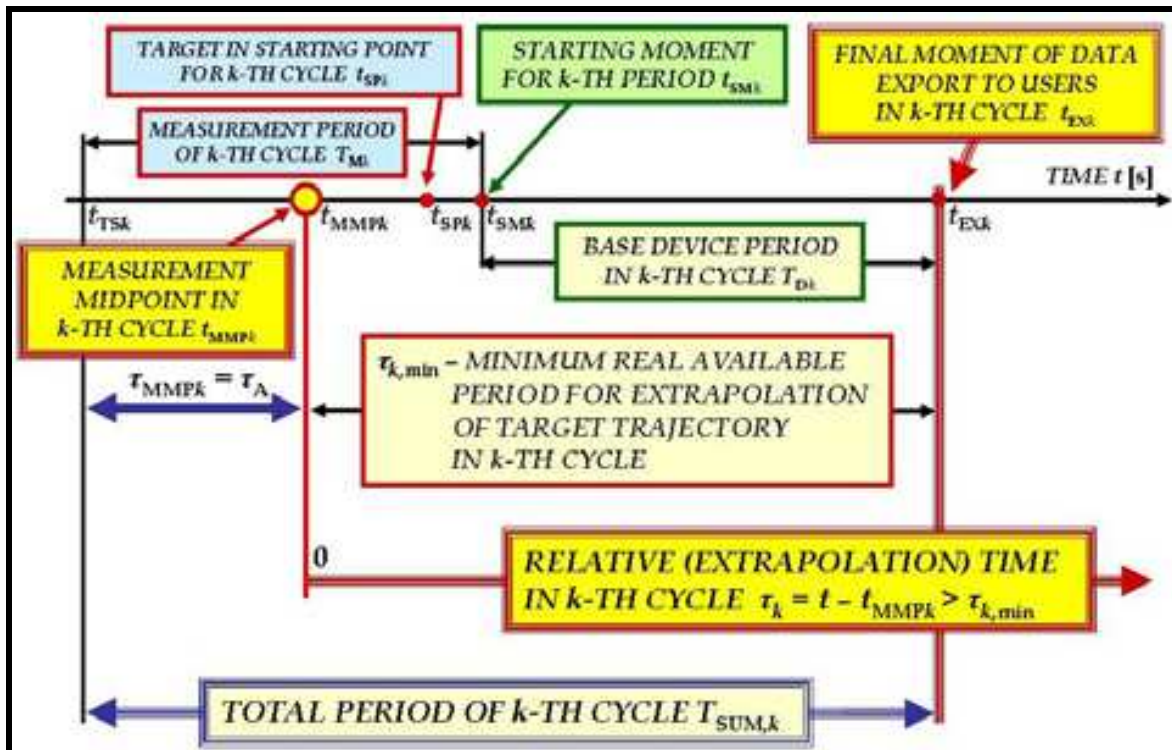


Fig. 15. Fundamental relations among time data useful for the target trajectory extrapolation

Two terms refer to the last record used in the k -th cycle. At the moment of taking the last stereo-pair images, the target point T lies at the starting point for the k -th cycle. The moment of export ending of the last record is denoted as the starting moment for the k -th cycle - Fig. 15. From the starting moment, all needful data for regress model processing is fully at disposal and can be evaluated.

Appropriate calculations and data export to users proceed during base device period in the k -th cycle T_{Dk} - Fig. 15. From the view of the user, the (total) device period in the k -th cycle $T_{DSk} = T_{Dk} + T_{DUk}$ consists of the base device period T_{Dk} and the user device period T_{DUk} , in which the user assumes data, executes preparatory operations and calculations, and only then he acquires extrapolated coordinates of the target for the time t . As it is evident from the Fig. 15, the time t must satisfy the condition of feasibility of extrapolation calculation in the k -th cycle $t > (t_{MMPk} + T_{DSk})$.

We have introduced the term measurement midpoint in the k -th cycle - Fig. 15. It is a point in the space, in which the target point T lies at the contractually selected moment t_{MMPk} . Linear regress model allows the estimate of coordinates $(E, N, H)_{TMMPk}$ of the target point and the estimate of the vector \mathbf{v}_{Tk} of the target speed in this point (or at the time t_{MMPk} respectively).

Input to linear regress model is created by coordinates in coordinate system of the base $(x, y, z)_{TBj}$ and corresponding times $t_j, j = j_{min}, \dots, j_{max}$. For notation simplification, we will use these denotations: $t_i, (x, y, z)_i, i = 1, 2, \dots, N_k$, so $i = 1$ corresponds to $j = j_{min}$, etc.

Furthermore, we will introduce common denotation q_i for x_i or y_i or z_i . For all three coordinates, it is valid the same linear regress model

$$\hat{q} = \hat{q}_0 + v_q \cdot \tau, \quad \tau = (t - t_1) \geq 0, \quad (4)$$

where (\hat{q}_0, v_q) are unknown parameters of linear regress model; the coefficient v_q has sense of coordinates of the speed vector $(v_{TBx}, v_{TBz}, v_{TBz})$.

The time for measurement midpoint is chosen (contractually – Fig. 15) as follows

$$t_{MMP,k} = t_{TS,k} + \tau_{MMP,k},$$

where $\tau_{MMP,k} = \tau_q + \Delta\tau_q, \quad \Delta\tau_q = t_{j_{min},k} - t_{TS,k}, \quad \tau_q = \frac{1}{N_k} \sum_{i=1}^{N_k} \tau_i, \quad \tau_i = t_i - t_1.$ (5)

Estimates of coordinates of measurement midpoint for the k -th cycle are then (q_{MMPk}) corresponds respectively to x_{MMPk} and y_{MMPk} and z_{MMPk}

$$q_{MMPk} = \hat{q}_0 + v_q \cdot \tau_q. \quad (6)$$

5. Simulation programs and Catalogue of targets

The principal purposes and characteristics of the simulation programs Test POERF and Test POERF RAW – including the Catalogue of targets – have been already introduced in the subsection 1.3.2.

The third version of the program Test POERF is described in (Cech & Jevicky, 2009c). Together four results, which have been obtained during simulations and which influence radically the solution of hardware and software of the passive optoelectronic rangefinder, are discussed here. (The four main results from the hitherto simulation experiments are presented inside the foregoing text.)

The Test POERF simulation program is an open development environment being continuously supplemented with further functions. We intend to upgrade radically the program in order to simulate the process of the moving target range measurement.

As mentioned before, the software package Test POERF RAW works with records from real scenes and consists of three separate programs: the editing program RAWedi, the main simulation program RAWdis and the viewer RAWpro.

The program RAWedi (Cech & Jevicky, 2010a) serves primarily to create horizontal stereo pair images of targets from shots that have captured wider area of a scene (a “standardization” of horizontal stereo pair images of targets and their nearest surroundings or the target image cut outs). These stereo pairs form a database part of the Catalogue of Targets. Simultaneously it allows editing stereo pair images for other purposes. The program is an analogy of the part of older program Test POERF, which is denoted as a generator of stereo pair images.

We have selected image formats REC (a special variant of RAW format) and BMP for images of the Catalogue of Targets (Cech & Jevicky, 2010a). The catalogue is a live system to which images of additional targets can be appended. For the present, we work with a database that was created from July to September 2009. The initial set has 76 stationary targets (buildings) and several other records with moving objects, especially vehicles. Meanwhile, we are dealing with stationary objects.

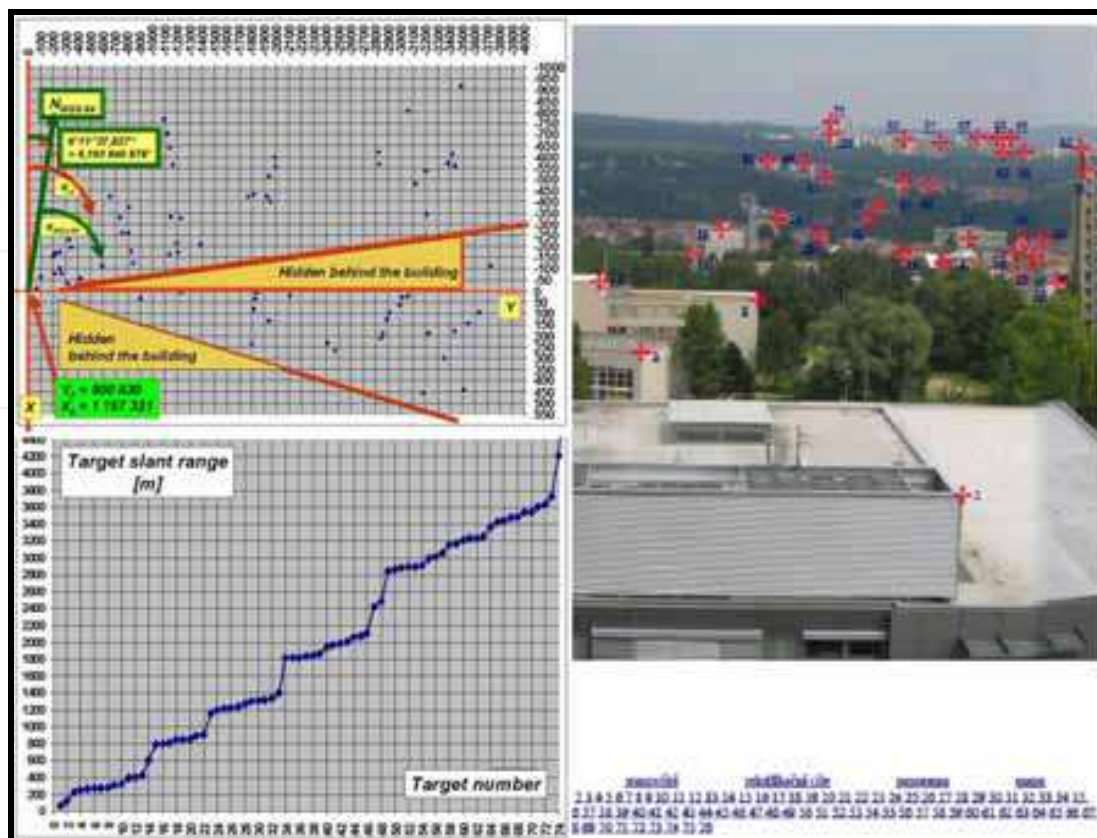


Fig. 16. Stationary targets registered in the Catalogue of Targets

Records of horizontal stereo pair shots of scenes were elected so that every target lies near to the centre of cameras field of view (suppression of possible distortion of objectives). Because of achievement of the record rate c. 10 image-pairs per second, the vertical binning was used, i.e. every two rows were aggregated into one row in all images (a special loss compression for RAW data); this compression technique does not influence the size of horizontal stereoscopic disparity.

Coordinates (X, Y) of every target and the POERF standpoint in the coordinate system of unified trigonometric cadastral network (S-JTSK) were determined with the use of Geographic information system (<http://nahlizenidokn.cuzk.cz>). Super-elevation angles of targets were measured by a theodolite – Fig. 16.

The program RAWdis (Cech & Jevicky, 2010b) that corresponds to the core of program Test POERF serves, as mentioned above, to determine the horizontal stereoscopic disparity of stereopairs from Catalogue of Targets (Fig. 17) and to estimate consequently the target slant range. We suppose that the simulation program RAWdis will be further developed and supplemented by new functions. The paper (Cech & Jevicky, 2010b) contains program outputs of the program version from May 2010. The problem of influences of front objects on the accuracy of the range measurement is also deeper discussed there (see the subsection 4.1 and the Figure 12).

Furthermore, in the paper there is a short problem specification of the influence of the spatial noise, whose source is partly the recording system (i.e. cameras, lenses and the basic digital image processing) and partly properties of the optical signal transmission channel – atmosphere (Roggeman & Welsh, 1996). The key role in the accuracy of the range measurement plays the atmospheric turbulence – (Rehor, 2004), (Cech et al., 2009a).

Adduced influences take effect in increasing the value of standard deviation σ_{CR} (see the subsection 4.1 and the Figure 11).

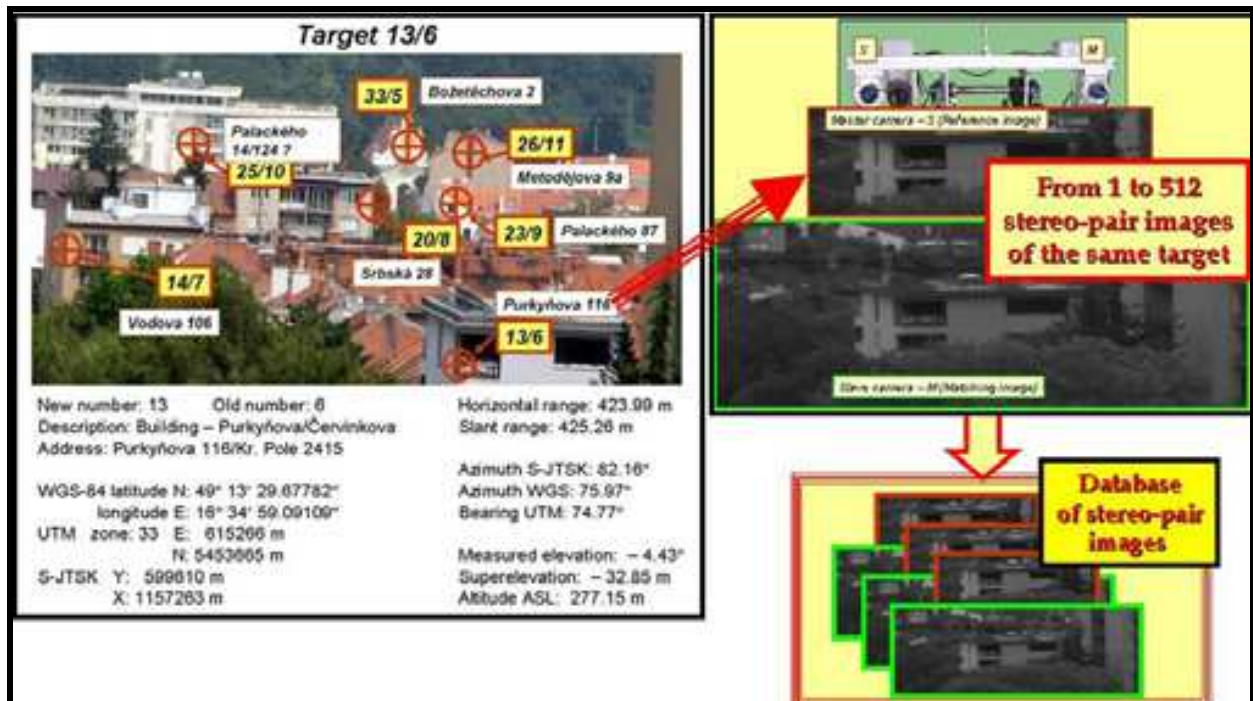


Fig. 17. The sample of "Catalogue card" for the target No. 13 from the Catalogue of Targets (it corresponds to a set stereo-pair shots in the Database of images)

6. Conclusion

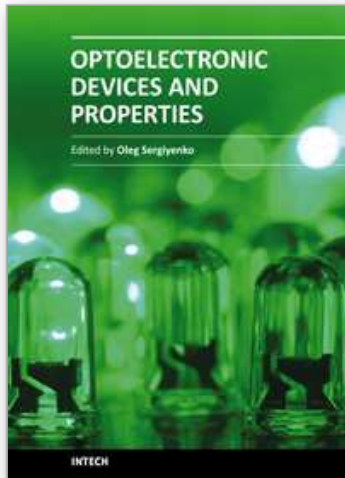
As it results from subsections 1.5 a 3.2, at the present we are working on the consequential project of the research and development of the passive optoelectronic rangefinder (the fourth period of the system development). In accordance with the project plan, we endeavor to solve progressively – on a qualitatively higher level – the problems mentioned in this chapter.

7. References

- Apotheloz, R. et al. (1981) *Oerlikon Taschenbuch*. Werkzeugmaschinenfabrik Oerlikon – Bühlerle A.G., Zürich, 706 p.
- Balaz, T.; Bucholcer, J.; Golian, M. & Racek, F. (1999) Probabilities of Target Discrimination. In *Proceedings of the 4th Conference on Weapon Systems*, Brno, May 1999, p. 203–207.
- Balaz, T. (2003) *Utilization possibilities of the passive optoelectronic rangefinder in current tank fire control systems*. (In Czech.) Habilitation dissertation. Military Academy in Brno, 2003. 139 p.
- Bouguet, J.-Y. (1999) *Pyramidal Implementation of the Lucas Kanade Feature Tracker*. Description of the algorithm. Intel Corp., Microprocessor Research Labs. Open CV Documents. From <http://sourceforge.net/projects/opencvlibrary>.
- Cech, V. & Jevicky, J. (2005) The Influence of Laser Rangefinder Parameters on the Hit Probability in Direct Tank Fire. In *Proceedings of 22nd International Symposium on*

- Ballistics*, Vancouver BC, Canada, 2005. DEStech Publications, vol. 1, p. 144-151. ISBN 1-932078-52-5.
- Cech, V.; Balaz, T.; Jevicky, J. & Racek, F. (2006) Analysis of Influence of Radiant Flux Distribution in the Laser Beam on the Probability of Right Target Range Measurement II. In *Proceedings of 40th International Conference Modeling and Simulation of Systems – MOSIS '06*. Prerov, 2006, p. 153-160. ISBN 80-86840-21-2.
- Cech, V. & Jevicky, J. (2007) The Development of Algorithms for Range Channel of the Passive Optoelectronic Rangefinder. In *Book of Extended Abstracts of Engineering Mechanics 2007 and Proceedings on CD-ROM*, Svratka, 2007, p. 27-28, ISBN 978-80-87012-06-2.
- Cech, V. et al. (2009a) *Research of high-end technologies and methods for recognition of moving objects, for determining of objects movement parameters and for automatic tracking systems of moving objects*. (In Czech.) Final research report of industrial research project of MIT CR FT – TA3/103. Oprox, a.s., Brno, 2009, 175 p., appendices 404 p.
- Cech, V. & Jevicky, J. (2009b) Algorithms of the Target Trajectory Extrapolation. In *Proceedings of 43rd Spring International Conference Modeling and Simulation of Systems – MOSIS '09*. MARQ, Roznov pod Radhostem, 2009, p. 144-153, ISBN 978-80-86840-45-1.
- Cech, V. & Jevicky, J. (2009c) Simulation of Target Range Measurement Process by Passive Optoelectronic Rangefinder. In *Proceedings of the First International Conference on Computational Intelligence, Modelling and Simulation*, Brno 2009, IEEE Computer Society 2009, p. 181-186, ISBN 978-0-7695-3795-5.
- Cech, V.; Jevicky, J. & Pancik, M. (2009d) Demonstration Model of Passive Optoelectronic Rangefinder. In *Recent Advances in Mechatronics 2008-2009*. Editors Brezina, T. and Jablonski, R., Springer-Verlag Berlin Heidelberg 2009, p. 79-84, ISBN 978-3-642-05021-3.
- Cech, V. & Jevicky, J. (2010a) Advanced Simulation of Range Channel of the Passive Optoelectronic Rangefinder. In *Proceedings of 44th Spring International Conference Modeling and Simulation of Systems – MOSIS ' X*. MARQ, Hradec nad Moravici, 2010, p. 101-108, ISBN 978-80-86840-51-2.
- Cech, V. & Jevicky, J. (2010b) Development of the Simulation Software Package Test POERF RAW. *Proceedings of the 7th EUROSIM Congress on Modelling and Simulation*. Prague, Czech Republic, September 6-10, 2010. Vol. 1: Book of Abstracts, p. 1. ISBN 978-80-01-04588-6. Vol. 2. Full Papers (CD), 10 pages, ISBN 978-80-01-04589-3.
- Composite authors (1958) *Naval Ordnance and Gunnery*. Volume 2, Fire Control, Chapter 16: Radar and Optics. Prepared by the Department of Ordnance and Gunnery United States Naval Academy. Edited and produced by the Bureau of Naval Personnel, NavPers 10798-A. U. S. Government Printing Office, Washington 25, D. C. From <http://editionwww.eugeneleeslover.com/USNAVY/CHAPTER-16-F.html>.
- Curti, P. (1945) *Einführung in die Äussere Ballistik*. Frauenfeld (Schweiz), Verlag Huber and Co. Aktiengesellschaft 1945, p. 408.
- Gebel, R. K. H. (1966) Optical Radar and Passive Opto-electronic Rangefinding. *The Ohio Journal of Science*, 66(5), pp. 496-507, ISSN 0030-0950.
- Gilligan, L. H. (1990) *Passive Range Finding Apparatus Utilizing Television Sensors*. US Patent No. 4 969 735, 13.11. 1990.

- Hänert, L. (1928) *Geschütz und Schuss. Eine Einführung in die Geschützmechanik und Ballistik*. Berlin, Verlag von Julius Springer 1928, 360 ps.
- Hanzl, V. & Sukup, K. (2001) *Photogrammetry I*. (In Czech.) University textbook. Brno University of Technology, FME. Academic press CERM, Brno 2001, 94 pages.
- Holst, G.C. (2000) *Electro-optical Imaging System Performance* (Second edition). JCD Publishing, Winter Park, FL, USA and SPIE Optical Engineering Press, Bellingham, WA, USA, 2000, 438 p.
- Jarvis, R. A. (1983) A Perspective on Range Finding Techniques for Computer Vision. *IEEE Transaction on Pattern Analysis and Machine Intelligence*, vol. PAMI-5, No. 2. March 1983, pp. 122-139, ISSN 0162-8828.
- Keprt, E. (1966) *Theory of optical apparatus IV: Theory and Construction of Optical Rangefinders*. (In Czech.) University textbook. Palacky University, Olomouc, Publication No. 1212 - 5331, 220 p.
- Kraus, K. (2000) *Photogrammetry*. Volume 1 - Fundamentals and Standard Processes. Dümmler, Köln, 397 p.
- Levine, M. D. et al. (1973) Computer determination of depth maps. *Computer Graphics Image Processing*, vol. 2, No. 4, pp. 134-150, Elsevier Science, ISSN 0146-664X.
- Rehor, Z. (2004) *Influences of the atmosphere on measuring by the passive optoelectronic system*. (In Czech.) Research report of industrial research project of MIT CR FD - K3/099 Research and development of technology and technical devices for both passive optoelectronic tracking and objects measuring. 1st chapter, 55 p., Oprox, a.s., Brno.
- Roggeman, M. C. & Welsh, B. (1996) *Imaging Through Turbulence*. CRC Press.
- Russell, I. (2001) Technical Transfer in the British Optical Industry 1888-1914: The Case of Barr and Stroud. *Scottish Industrial History*, 21, pp. 15-33.
- Scharstein, D. & Szelisky, R. (2002) A Taxonomy and Evaluation of Dense Two-Frame Stereo Correspondence Algorithms. *International Journal of Computer Vision*, 47 (1-3), pp. 7-42, ISSN 0920-5691.
- Skvarek, J. et al. (2004) *Research and development of technology and technical devices for both passive optoelectronic tracking and objects measuring*. (In Czech.) Abbreviated final research report of industrial research project of MIT CR FD - K3/99. Oprox, a.s., Brno. Epitome 50 p.
- Uherik, L. et al. (1985) *Small arms aiming*. (In Czech.) Study for ZVS-VVU Brno, government research project SRAZ A/02. VAAZ, Brno, 103 p.
- Wallis, D. A. (2005) History of Angle Measurement. Proceedings of *From Pharaohs to Geoinformatics*. FIG Working Week 2005 and GSDI-8, Cairo, Egypt, April 2005, 17 p.
- Zitnick, C. L. & Kanade, T. (2000) A Cooperative Algorithms for Stereo Matching and Occlusion Detection. *IEEE Transactions on Pattern Analysis and Machine Intelligence*, vol. 22, No. 7, July 2000, pp. 675-684, ISSN 0162-8828.



Optoelectronic Devices and Properties

Edited by Prof. Oleg Sergiyenko

ISBN 978-953-307-204-3

Hard cover, 660 pages

Publisher InTech

Published online 19, April, 2011

Published in print edition April, 2011

Optoelectronic devices impact many areas of society, from simple household appliances and multimedia systems to communications, computing, spatial scanning, optical monitoring, 3D measurements and medical instruments. This is the most complete book about optoelectromechanic systems and semiconductor optoelectronic devices; it provides an accessible, well-organized overview of optoelectronic devices and properties that emphasizes basic principles.

How to reference

In order to correctly reference this scholarly work, feel free to copy and paste the following:

Vladimir Cech and Jiri Jevicky (2011). Research and Development of the Passive Optoelectronic Rangefinder, Optoelectronic Devices and Properties, Prof. Oleg Sergiyenko (Ed.), ISBN: 978-953-307-204-3, InTech, Available from: <http://www.intechopen.com/books/optoelectronic-devices-and-properties/research-and-development-of-the-passive-optoelectronic-rangefinder>

INTECH
open science | open minds

InTech Europe

University Campus STeP Ri
Slavka Krautzeka 83/A
51000 Rijeka, Croatia
Phone: +385 (51) 770 447
Fax: +385 (51) 686 166
www.intechopen.com

InTech China

Unit 405, Office Block, Hotel Equatorial Shanghai
No.65, Yan An Road (West), Shanghai, 200040, China
中国上海市延安西路65号上海国际贵都大饭店办公楼405单元
Phone: +86-21-62489820
Fax: +86-21-62489821

© 2011 The Author(s). Licensee IntechOpen. This chapter is distributed under the terms of the [Creative Commons Attribution-NonCommercial-ShareAlike-3.0 License](#), which permits use, distribution and reproduction for non-commercial purposes, provided the original is properly cited and derivative works building on this content are distributed under the same license.

IntechOpen

IntechOpen